Nuclear Engineering and Design 333 (2018) 16–24

Contents lists available at ScienceDirect

Nuclear Engineering and Design

journal homepage: www.elsevier.com/locate/nucengdes

Measurement of the residual stresses in a PWR Control Rod Drive Mechanism nozzle

H.E. Coules*, D.J. Smith[1]

Department of Mechanical Engineering, University of Bristol, Bristol, UK

ARTICLE INFO

Keywords:
Residual stress
Deep Hole Drilling
Pressurised Water Reactor
Cladding
Control Rod Drive Mechanism

ABSTRACT

Residual stress in the welds that attach Control Rod Drive Mechanism nozzles into the upper head of a PWR reactor vessel can influence the vessel's structural integrity and initiate Primary Water Stress Corrosion Cracking. PWSCC at Alloy 600 CRDM nozzles has caused primary coolant leakage in operating PWRs. We have used Deep Hole Drilling to characterise residual stresses in a PWR vessel head. Measurements of the internal cladding and nozzle attachment weld showed that although modest tensile stresses occur in the cladding, the attachment weld contains tensile residual stresses of yield magnitude. Despite the large dispersion of residual stress data for nozzle attachments of this type, all available data suggest that assuming a residual stress profile bounded by the weld material's yield stress would be conservative for assessment purposes.

1. Introduction

The upper head of the Reactor Pressure Vessel (RPV) in a Pressurised Water Reactor (PWR), contains an arrangement of set-in nozzles which penetrate through the vessel head (see Fig. 1) and accommodate the Control Rod Drive Mechanism (CRDM). Most operational PWRs have been built with CRDM nozzles of a similar design: an Alloy 600 tube with a 4-in. outer diameter shrink-fitted into a hole in the vessel upper head and welded at the vessel interior with Alloy 182 (Fig. 2).

Some Alloy 600 nozzle penetrations have experienced problems relating to contact with the borated primary cooling water used in PWRs (Grimmel, 2005). Firstly, Primary Water Stress Corrosion Cracking (PWSCC) can occur in the Alloy 600 tube itself and cause axial-radial cracks. This type of cracking was first observed in the French Bugey 3 reactor in 1991, and since then numerous cases have occurred on PWRs worldwide (Gorman et al., 2009; Hwang, 2013; IAEA, 2011; Kang et al., 2014). Although axial-radial cracks in the nozzle are not a direct risk to pressure vessel integrity, they may allow low-level leakage of the primary coolant (Calvar and Curieres, 2012; Rudland et al., 2004). A small leak at a nozzle can cause primary coolant to come into contact with the carbon steel of the pressure vessel wall and corrode it (Grimmel, 2005). This was the cause of a case of severe corrosion observed at the Davis-Besse power plant in 2002 (NRC, 2002). Secondly, PWSCC which results in circumferential cracking in the nozzle (or in the Alloy 182 weld material surrounding it) could cause a risk of nozzle breakage or ejection and a consequent Loss-Of-Coolant Accident (LOCA) (Calvar and Curieres, 2012). Circumferential cracks of this type were first reported in the early 2000s at several reactors in the USA, leading to nozzle replacement (Grimmel, 2005). Thirdly, PWSCC can occur in the Alloy 182 weld material of the circumferential weld which attaches the nozzle tube at the internal surface of the pressure vessel head (Gorman et al., 2009). This can allow primary coolant leakage into the interference fit region between the tube and pressure vessel wall, and subsequently out of the top to the nozzle attachment (Grimmel, 2005; Crawford et al., 2012).

Residual stresses which exist in the nozzle, weld and surrounding region are significant for two reasons: they affect the rate at which corrosion cracks grow and they affect the initiation of fracture from existing corrosion cracks. Specific areas of concern are the inner diameter of the nozzle tube and in the weld metal in the circumferential weld, since the presence of tensile residual stresses at these locations could promote PWSCC. Several processes during nozzle manufacture are known to cause significant residual stresses: internal cladding of the vessel head, shrink-fitting the Alloy 600 tube into the vessel and J-groove welding of the tube at the internal surface (IAEA, 1999). As a result, the final residual stress state is complex and difficult to predict reliably using finite element analysis.

In this study we aim to experimentally characterise the residual stresses deep inside a CRDM nozzle attachment weld. This will provide a typical reference case against which other experimental and model residual stress profiles can be compared, and allow us to recommend

* Corresponding author.
E-mail address: harry.coules@bristol.ac.uk (H.E. Coules).
[1] Deceased.

https://doi.org/10.1016/j.nucengdes.2018.04.002
Received 11 December 2017; Received in revised form 30 March 2018; Accepted 2 April 2018

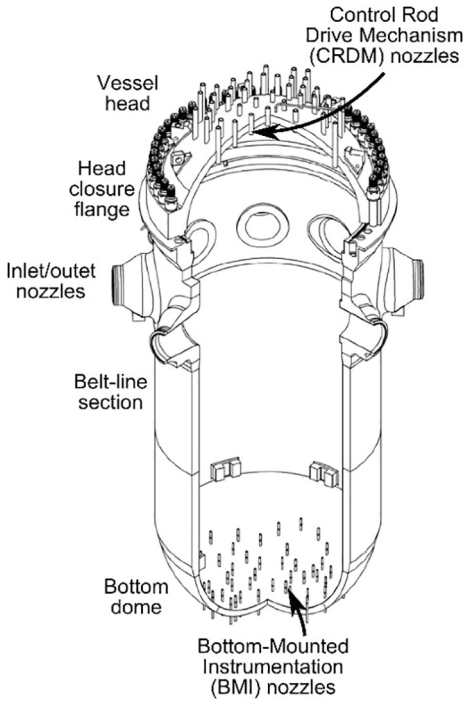

Fig. 1. Location of the CRDM nozzles on a PWR reactor pressure vessel.

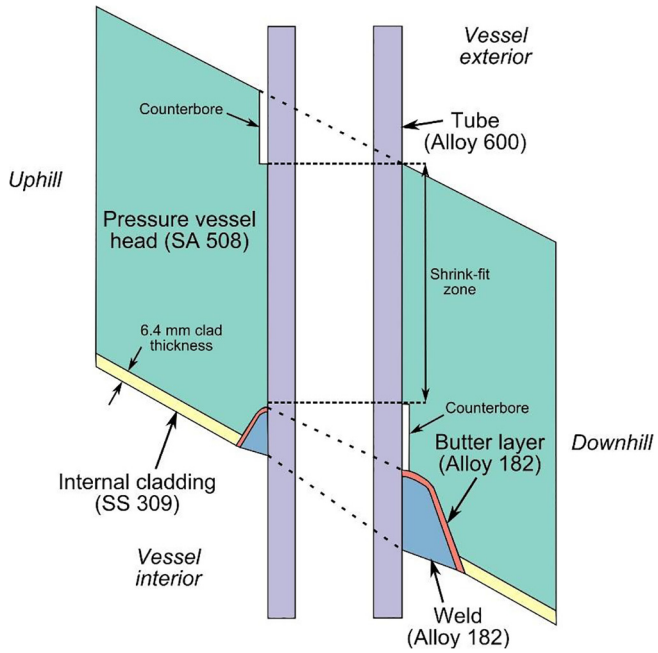

Fig. 2. Cross-sectional schematic of a CRDM nozzle and surrounding region of the pressure vessel head. Adapted from Anderson et al. (2008) and Rudland et al. (2004). Not to scale, disparity in weld sizes exaggerated.

how residual stresses should be considered in the analysis of cracks in the attachment weld and nozzle tube.

2. Measurements

2.1. Specimen

The specimen is a section of a PWR upper pressure vessel head containing three CRDM nozzles, as shown in Fig. 3. It was flame-cut from the complete pressure vessel head before shipping to the measurement laboratory. The pressure vessel head was manufactured by Babcock & Wilcox for the cancelled Washington Nuclear Power plant (WNP-1&4) and never used in an operating reactor. Although no B&W "205-design" 2-loop reactors like the one that this specimen was intended for were completed in the USA, the CRDM penetration design is essentially identical to that found in many PWRs currently in operation.

The specimen contains three CRDM nozzles, numbered 61, 80 and 81 (see Fig. 3a). Nozzle #61 is at an angle of 31° to the perpendicular of the internal surface of the specimen, whereas Nozzles #80 and #81 are at 40°. The thickness of the pressure vessel head is 203 mm, including the interior cladding. The CRDM nozzles pass through a greater thickness of material since they do not run perpendicular to the surface. The wall thickness in the axial direction of Nozzle #61 is 237 mm and the thickness in the axial direction of Nozzles #80 and #81 is 265 mm. Fig. 2 shows a cross-sectional view of a nozzle. The nozzle tube is made of an Inconel 600 pipe, whereas the pressure vessel head is forged ASME SA 508 Grade 3 ferritic steel cladded on the interior with AISI 309 austenitic stainless steel using Submerged Arc Welding (SAW). During manufacture, the vessel head is drilled and counterbored, leaving an internal section where shrink-fitting is possible. The nozzle tube is dipped in liquid nitrogen and inserted to achieve the shrink-fit. A J-groove weld using Inconel 182 is used to attach the tube at the vessel interior. The cross-sectional area of the weld is larger on the downhill side of the weld; the greater volume of contracting weld metal here has been known to cause bending or ovalisation of the tube (IAEA, 1999), although that was not observed on the specimen used in this study.

2.2. Deep Hole Drilling measurements

Residual stress measurements were performed using the Incremental Deep Hole Drilling (IDHD) method (Mahmoudi et al., 2009). In this process, a through-hole of 1.5 or 3 mm diameter (the 'reference hole') is drilled into the specimen using a gun drill. The profile of the hole is measured throughout its length using an air probe. Next, a circular trepan is cut concentric to the reference hole using Electrical Discharge Machining (EDM). The trepan is sunk incrementally and at each increment of depth, the reference hole is re-measured. As it progresses, the trepan releases the residual stress in a cylindrical core of material surrounding the reference hole. The residual stress that initially existed along the line of the reference hole prior to trepanning can be calculated from the reference hole profile measurements.

The analysis used for determining residual stresses from measured diametral distortions and the assumptions of this analysis are described by George et al. (2002) and Kingston (2003), Kingston et al. (2006). For a circular hole in an infinite thin elastic plate subjected to a remotely-applied uniform stress, the diametral strain ε_θ is defined as:

$$\varepsilon_\theta(\theta) = \frac{\Delta d(\theta)}{d_0(\theta)} \tag{1}$$

where Δd is the change in hole diameter and d_0 is the original diameter. All three quantities are a function of the angle θ on the circumference of the hole (defined as anticlockwise from the x-axis). The diametral strain can be related to the applied stress by:

$$\varepsilon_\theta(\theta) = \frac{1}{E}(\sigma_{xx} f(\theta) + \sigma_{yy} g(\theta) + \tau_{xy} h(\theta)) \tag{2}$$

where σ_{xx}, σ_{yy} and τ_{xy} are components of the stress tensor and E is the Young's modulus of the (isotropic) material. The functions $f(\theta)$, $g(\theta)$, $h(\theta)$ are:

$$\begin{aligned} f(\theta) &= 1 + 2\cos(2\theta) \\ g(\theta) &= 1 - 2\cos(2\theta) \\ h(\theta) &= 4\sin(2\theta) \end{aligned} \tag{3}$$

The diametral strain at n different angles can be represented by the

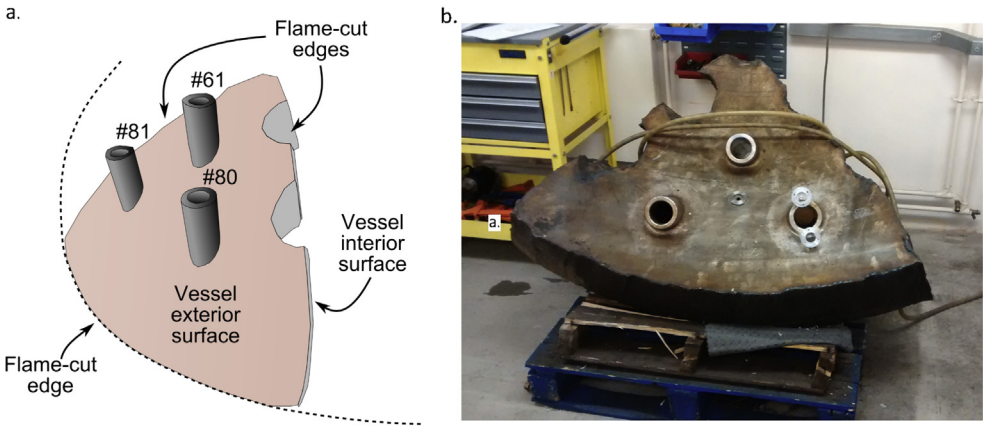

Fig. 3. PWR pressure vessel head section. (a) Schematic view from the exterior showing nozzle numbering. (b) Specimen positioned for residual stress measurement, showing interior surface.

Table 1
Typical elastic properties of CRDM nozzle materials (Fredette, 2011; ASM Metals Handbook, 1980; Peckner and Bernstein, 1977; ASME Boiler and Pressure Vessel Code, 2001).

Material	Young's modulus (GPa)	Poisson ratio
SA508	192	0.3
SS309	200	0.30
Alloy 600	207–214	0.29–0.32
Alloy 182 (as-deposited condition)	156	0.3

following column vector:

$$\varepsilon_i = [\varepsilon_\theta(\theta_1), \varepsilon_\theta(\theta_2), ..., \varepsilon_\theta(\theta_n)]^T \quad (4)$$

and the applied stress can also be represented in column vector form:

$$\sigma_i = [\sigma_{xx}, \sigma_{yy}, \tau_{xy}]^T \quad (5)$$

This allows Eq. (2) to be written as the system of simultaneous linear equations:

$$\varepsilon_i = M_{ij}\sigma_j \quad (6)$$

where:

$$M_{ij} = \frac{1}{E}\begin{bmatrix} f(\theta_1) & g(\theta_1) & h(\theta_1) \\ f(\theta_2) & g(\theta_2) & h(\theta_2) \\ \vdots & \vdots & \vdots \\ f(\theta_n) & g(\theta_n) & h(\theta_n) \end{bmatrix} \quad (7)$$

At each position along the length of a DHD reference hole, measurements of the diametral strain ε_θ caused by residual stress relaxation during trepanning are taken at n angles. In all measurements performed in this study $n = 8$, with measurement angles at 22.5° increments. The residual stress is then determined by solving Eq. (6) in a least-squares sense by taking the pseudo-inverse of M_{ij}. This process is repeated for each location along the length of the reference hole, yielding a depth-resolved measurement of three components of the stress tensor. In this study, depth-resolved representative elastic properties for each of the specimen materials encountered by the reference hole were used in Eq. (7); these are summarised in Table 1.

The analysis described above assumes that the region surrounding the reference hole (i.e. the trepan core) undergoes only elastic deformations during trepanning. However, in specimens containing residual stresses of a magnitude approaching the yield stress of the material, the stress concentration caused by the trepan can cause plastic deformation during trepanning (Hossain et al., 2012; Mahmoudi et al., 2011). In the Incremental Deep Hole Drilling (IDHD) method, measurements of the reference hole diametral strain are taken at every increment of trepanning depth. The variation in strain as a function of trepan depth can be used to indicate and correct for the occurrence of inelastic deformation.

Measurements were taken at three locations on the specimen. One measurement location was in-between the three nozzles and equidistant from each – this was used to indicate the residual stress resulting from the internal cladding process alone and so is referred to as the "clad" measurement. For the clad measurement, the reference hole was drilled

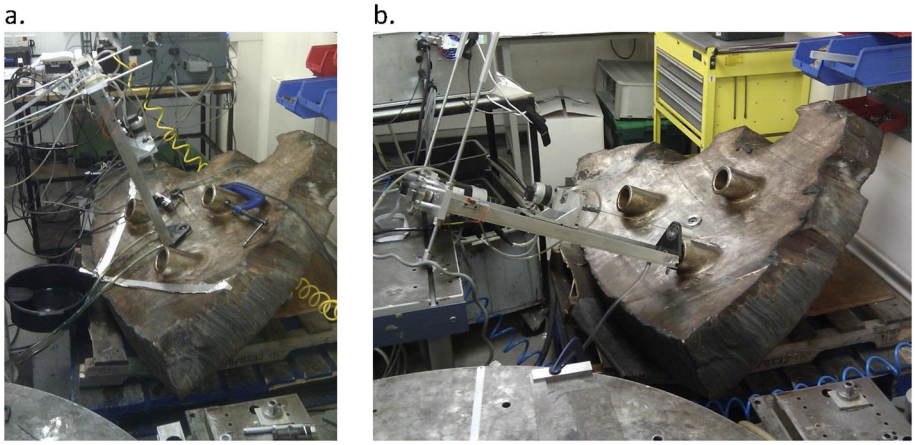

Fig. 4. Air-probe measurements being performed at (a) the central 'clad' location, (b) the Nozzle #80 'uphill' location. Note the different reference hole angles with respect to the pressure vessel internal surface.

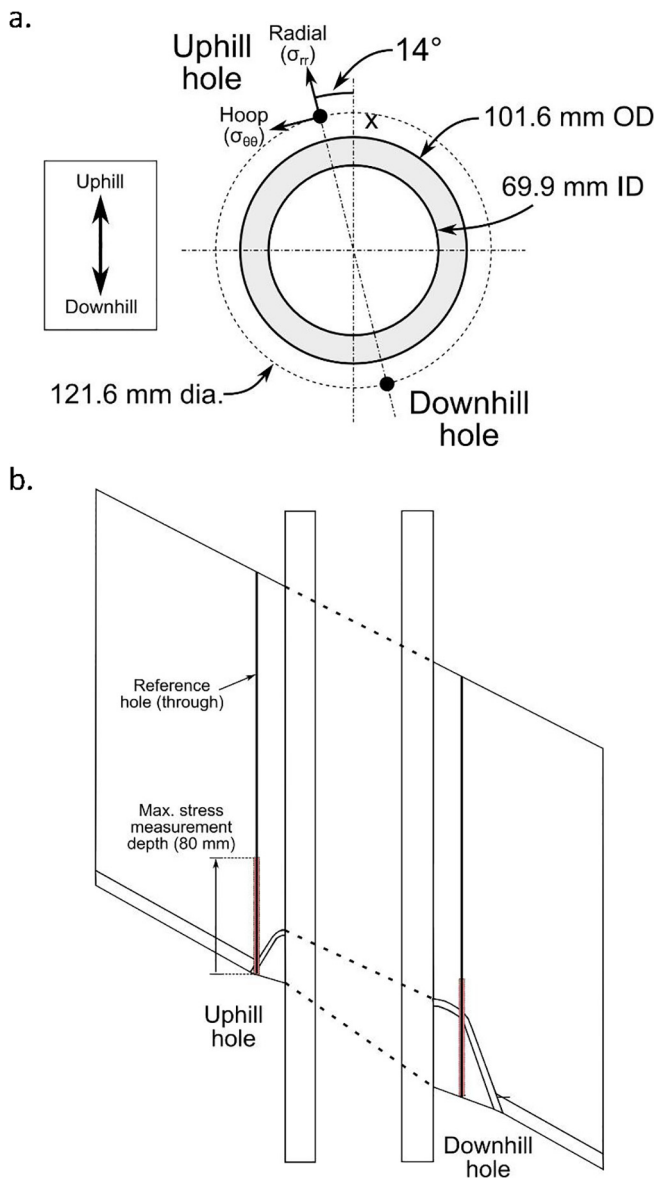

Fig. 5. (a) Locations of the two IDHD measurement around Nozzle #80. The IDHD reference holes are parallel to the nozzle axis and 20 mm from its outer diameter. (b) Cross-sectional view showing drilling and trepanning depths (nB. not to scale, disparity in weld sizes exaggerated).

perpendicular to interior surface of the pressure vessel (see Fig. 4a), and the residual stress distribution through the specimen was measured to a depth of 170 mm. The clad measurement was made using a reference hole of 3 mm diameter and an EDM trepan of 10 mm diameter.

The other two measurements were made at Nozzle #80. The reference holes for these two measurements were drilled parallel to the axis of the nozzle (see Fig. 4b), i.e. at an angle of approximately 40° to the internal surface of the specimen. The measurement locations were on opposite sides of the nozzle and at a radius of 60.8 mm from its axis (i.e. 10 mm from the nozzle OD). Viewed from the vessel interior, the 'uphill' hole was offset 14° anticlockwise from the vessel head's uphill direction, and the 'downhill' hole was offset likewise (Fig. 5a). At these locations, residual stress measurements were made to a depth of 80 mm (Fig. 5b). The nozzle IDHD measurements were both performed using a reference hole diameter of 1.5 mm and a EDM trepan diameter of 5 mm.

To facilitate the two IDHD measurements at Nozzle #80, a section containing the nozzle and surrounding weld was cut from the main specimen using four bandsaw cuts parallel to the nozzle axis. Fig. 6 shows the nozzle section before and after extraction. The uphill IDHD hole was air-probed to a depth of 170 mm before and after cutting-out of the nozzle section to check whether the cutting operation altered the residual stress state at the measurement locations significantly.

The parameters used for the three IDHD measurements are summarised in Table 2. The trepan depths were based on initial estimates of the through-depth gradient in residual stress: a greater number of trepan increments was used where the stress gradient was believed to be higher, to ensure that any plastic relaxation of stress would be detected. For example, since a steep gradient in residual stress close to the surface was expected in the clad measurement, incremental trepanning was only performed to a depth of 10 mm.

Typical diametral measurements of a reference hole are shown in Fig. 7. Fig. 7a shows that directly after drilling, the reference hole has a measurable variation in diameter over its depth – this is a normal result of the gun-drilling process. However, residual stresses are calculated using the change in diameter before and after trepanning, and initial diametral non-uniformity has a minimal effect on the measured change in diameter (see Fig. 7b).

3. Results

3.1. Clad measurement

Fig. 8 shows residual stress relaxation after six increments of trepanning at the clad measurement location. As the trepan is cut, the residual stress gradually relaxes. The result after trepanning the full depth of the measurement hole is shown in black. The indicated stress observed during incremental trepanning never exceeds the final stress distribution, indicating that no significant plastic deformation has occurred during the trepanning process. This is unsurprising given the relatively low residual stresses in the clad. Consequently, the final elastically-calculated measurement is reliable and does not require plasticity correction.

The residual stress distribution in the clad (Fig. 9b) is characteristic for a clad of this type: tensile in the cladding metal, compressive below the clad and almost equi-biaxial. The near-surface residual stress profile is qualitatively similar to that measured in similar PWR vessel clads (Sattari-Far and Andersson, 2006). The peak tensile stress in the clad of approximately 150 MPa observed here is also comparable to previous measurements, although a great deal of scatter exists in published data. The residual stress profile throughout the rest of wall thickness (Fig. 9a) shows some variations but these are restricted to less than 70 MPa in magnitude. This variation may be due to forging stresses which persist to a small degree after heat treatment.

3.2. Extraction of nozzle #80

Diametral measurements of the 'uphill' hole before and after extraction of Nozzle #80 from the complete specimen (see Fig. 6), were used to determine the residual stress relaxation that occurred during extraction. Fig. 10 shows that the magnitude of residual stress relaxation is less than 40 MPa over most of the measured depth of the uphill hole. Therefore, cutting-out of the nozzle section only caused small changes in the residual stress state in the weld prior to the nozzle IDHD measurements.

3.3. Measurements at nozzle #80

As in the clad measurement Fig. 8, the residual stresses in both the uphill and downhill measurement cores at the Nozzle #80 attachment weld were observed to relax incrementally during trepanning (see Fig. 11). This indicates that plastic deformation of the DHD core during trepanning was negligible and so the elastic analysis described in Section 2.2 can be used.

The residual stress state at the uphill and downhill nozzle locations

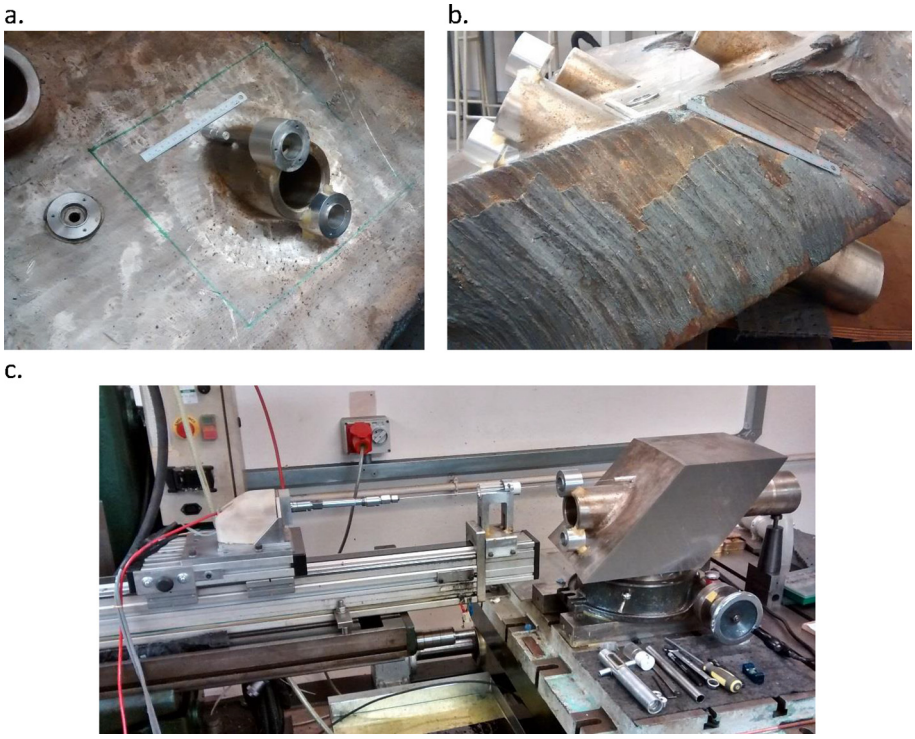

Fig. 6. A section of pressure vessel head containing Nozzle #80. (a) Before extraction, viewed from interior side. (b) Before extraction, viewed from side of nozzle. (c) After extraction, during air-probe measurement of the uphill hole.

Table 2
Summary of IDHD measurement parameters.

Measurement	Reference hole dia. (mm)	Nominal trepan core dia. (mm)	Nominal trepan depths (mm)
Clad	3	10	2, 4, 6, 8, 10, thru
#80 Uphill	1.5	5	5, 10, 20, 30, 40, 50, 60, 70, 80, 100
#80 Downhill	1.5	5	5, 10, 20, 30, 40, 50, 60, 70, 80, 100

is shown in Fig. 12. Strongly tensile residual stresses exist in the weld in both the hoop and radial directions. However, the greater volume of weld material at the downhill side of the nozzle causes a higher tensile stress peak here than on the uphill side – up to 380 MPa (at 7.5 mm below the surface). The peak tensile stress in the downhill side of the weld is approximately at the yield stress of the Alloy 182 weld metal (Jang et al., 2008).

4. Discussion

4.1. Residual stress profiles and uncertainty

Fig. 12 shows that tensile residual stresses of yield magnitude were exist in the CRDM nozzle attachment weld. This contrasts with relatively small residual stresses (approx. 150 MPa) in the surrounding pressure vessel internal cladding. In both the clad and the CRDM nozzle (Figs. 9 and 12, respectively), significant residual stresses were only observed in surface zones affected by cladding and welding – not deep within the pressure vessel wall. Any residual stresses resulting from deformation of the ferritic steel vessel wall during forging or during nozzle shrink-fitting appear to have been relaxed.

The shrink-fitting operation used to fit the nozzle into the vessel head was expected to cause tensile hoop stress below the welds at both measurement locations, since the measurement holes are only 10 mm from the shrink-fit interface. However, no tensile stresses characteristic of shrink-fitting are seen in the residual stress distributions in Fig. 12. In fact, on both sides of the nozzle, the residual stress is lower than 30 MPa

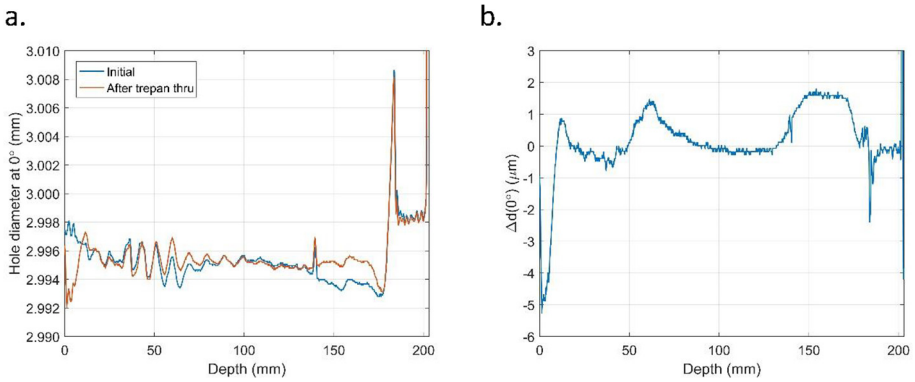

Fig. 7. Typical diametral measurements, from the 'clad' measurement hole at 0°. (a) Measured diameter of the measurement hole at 0° before and after trepanning. (b) Change in hole diameter at 0°.

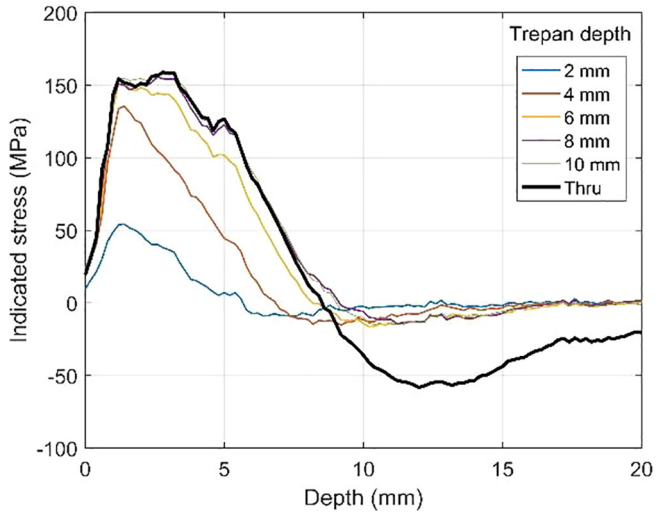

Fig. 8. Residual stress relaxation at the clad measurement location after six increments of trepanning. Stress in the uphill-downhill direction (σ_{xx}) is shown.

beyond 50 mm depth (i.e. beyond the weld bead). Again, this strongly suggests that any stresses introduced by shrink-fitting may be relaxed during subsequent heat treatment.

The uncertainty in the IDHD measurements is difficult to estimate without an independent reference measurement. A study by George et al. (2002) suggests an uncertainty of ± 30 MPa would be reasonable for the technique and materials used in the nozzle measurements. This agrees with the observed scatter measurement well beyond the trepanned depth, i.e. of non-stress-relieved parts of the DHD core, which can be seen in Fig. 11. The parameters used in the clad measurements are similar to those used by Goudar et al. (2011), who used error analysis to estimate uncertainty at ± 10–15 MPa. This is also in agreement with the observed scatter for repeat hole profile measurement of the clad DHD core.

4.2. Comparison of residual stresses in CRDM nozzle attachments

Fig. 13 shows a comparison of through-thickness distributions of residual hoop stress in CRDM nozzle attachment welds taken from different sources. One other DHD measurement (of a nozzle mock-up which penetrates perpendicular to a clad plate representing the vessel wall) has been reported by Katsuyama et al. (2010); the other results are predictions from finite element modelling of the welding process. The models that were used to generate the results reported by Rudland et al. (2007) do not incorporate heat treatment of the nozzle, and so some stress relaxation relative to these data would be expected. Although all sources report strongly tensile stresses in the weld metal, there is broad scatter between the results. This can be partly attributed to the different nozzle geometries investigated by the different researchers, and to the inherent difficulty in modelling this complex welding process accurately. The two experimental DHD results agree relatively well for the uphill side of the nozzle, where the volume of weld metal for the two geometries is most similar. However, on the downhill side there is a disparity of > 200 MPa in the weld metal; this is most likely due to differences in the weld geometry and materials used. All sources show the hoop stress reducing to approximately zero beyond 40–50 mm, i.e. beyond the weld metal.

4.3. Consequences for structural integrity analysis

PWSCC in CRDM nozzles typically initiates at the ID of the Alloy 600 nozzle tube, but can also initiate in the Alloy 182 CRDM attachment weld (Gorman et al., 2009). In this study, residual stress measurements were made directly outside the nozzle tube, in the attachment weld. Although residual stresses measured here will not be representative of the stress state at the most likely location of Alloy 600 cracking initiation, they can be used to validate models of the welding process which predict the stress state that the nozzle tube ID. Finite element models of the CRDM attachment weld have been used to predict the residual stress state in the weld and nozzle in many previous studies (Kang et al., 2014; Anderson et al., 2008; Rudland et al., 2007; Bae et al., 2014; Wilkowski et al., 2006), including those shown in Fig. 13, and the results can be used for fracture analysis of PWSCC cracks (Katsuyama et al., 2010; Rudland et al., 2005; Udagawa et al., 2010).

Although weld models of CRDM attachments are generally difficult to validate due to the lack of experimental residual stress measurements from comparable welds, the data given here could be used to validate future CRDM weld models. In principle, it could also be used directly for fracture mechanics analysis of cracks in the Alloy 182 attachment weld using the weight function method (Rudland et al., 2004), or for analysis of PWSCC growth rates (Gorman et al., 2009). However, the dispersion of residual stress data from different sources is large (see Fig. 13). Therefore this data should not be used directly when performing structural integrity assessment on similar CRDM nozzles for which the residual stress distribution is unknown. Some fracture-mechanics-based assessment procedures, such as EDF Energy's R6 procedure (R6: Assessment of the Integrity of Structures Containing Defects, Revision 4, Amendment 11, 2015), provide upper-bound estimates of the residual stress distribution for certain weld types. For instance, in R6 the hoop stress in a set-in nozzle across the same sections as used here for DHD measurement (see Fig. 5b) can be assumed to be uniformly tensile, at the level of the parent or weld metal yield strengths – whichever is greater. For this nozzle attachment weld, a uniform stress

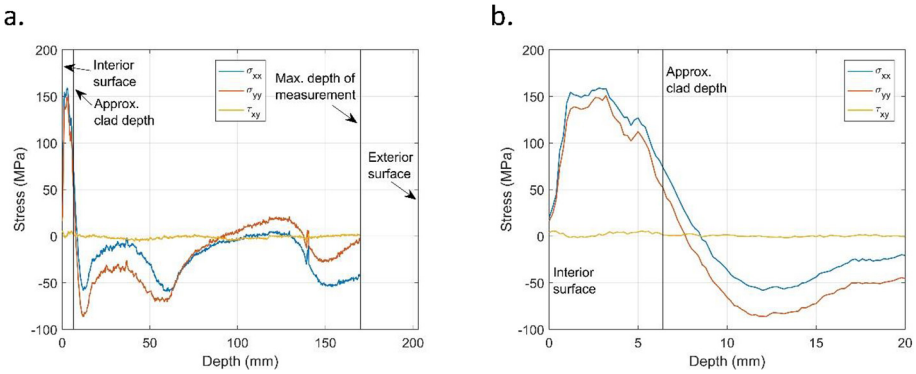

Fig. 9. Residual stress at the clad measurement point (i.e. remote from the CRDM nozzles) as a function of through-wall depth. (a) Stress variation across the whole measured depth. (b) Close-up view of the residual stress distribution at the interior surface. σ_{xx} is in the uphill direction of the pressure vessel head, σ_{yy} is the circumferential direction.

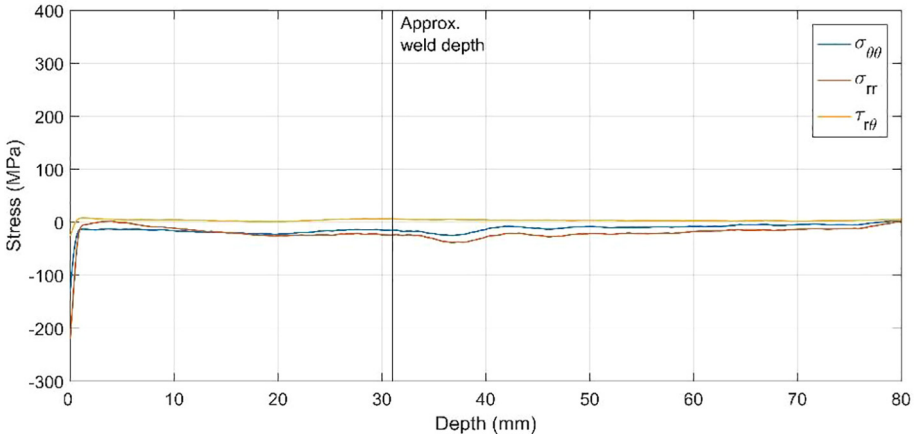

Fig. 10. Residual stress relaxed at the uphill measurement hole during extraction of Nozzle #80. Measurement coordinate system is defined in Fig. 5a.

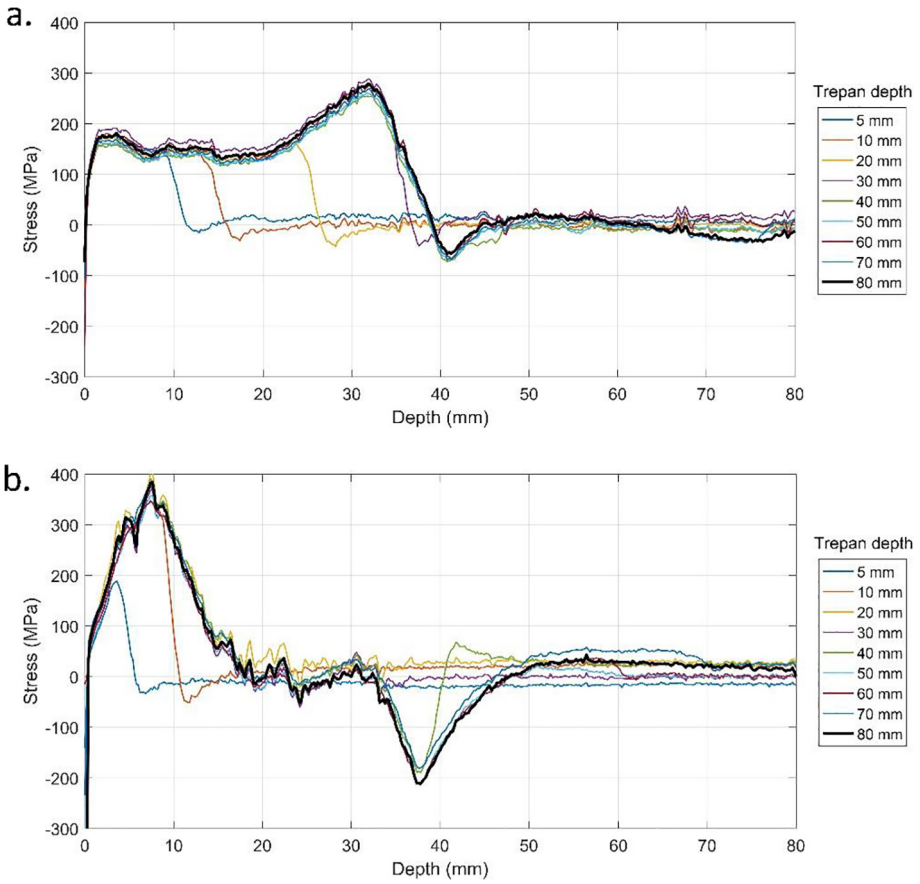

Fig. 11. Residual stress relaxation at nozzle measurement locations ($\sigma_{\theta\theta}$ component only shown) during incremental trepanning. (a) Uphill measurement location. (b) Downhill measurement location.

of 552 MPa (weld metal yield strength at room temperature) would be used. As shown in Fig. 13, this does indeed provide a conservative bound to all of the measured and predicted hoop stress data.

Despite design changes and repair/mitigation programmes, PWSCC of CRDM nozzles in existing PWRs is an ongoing issue (Gorman et al., 2009; IAEA, 2011; Kang et al., 2014). Prediction of the residual stress state in CRDM nozzles is challenging due to a combination of complex weld geometry, materials and lack of calibration data. Furthermore, residual stress measurement in these components is difficult due to their large size and because the presence of multiple materials complicates the use of diffraction-based methods.

5. Conclusions

The residual stresses in a PWR vessel section have been characterised experimentally. The internal stainless steel cladding contains equi-biaxial tensile stress with a magnitude of 150 MPa, which is well below the yield strength of the cladding material. The CRDM nozzle attachment weld contains strongly tensile and biaxial residual stresses. The highest residual stresses, of approximately yield magnitude, were measured on the downhill side of the nozzle where there is a greater volume of weld material. Although the presence of large tensile residual stresses in the CRDM attachment weld was expected, it highlights the need to take residual stress into account in the structural integrity

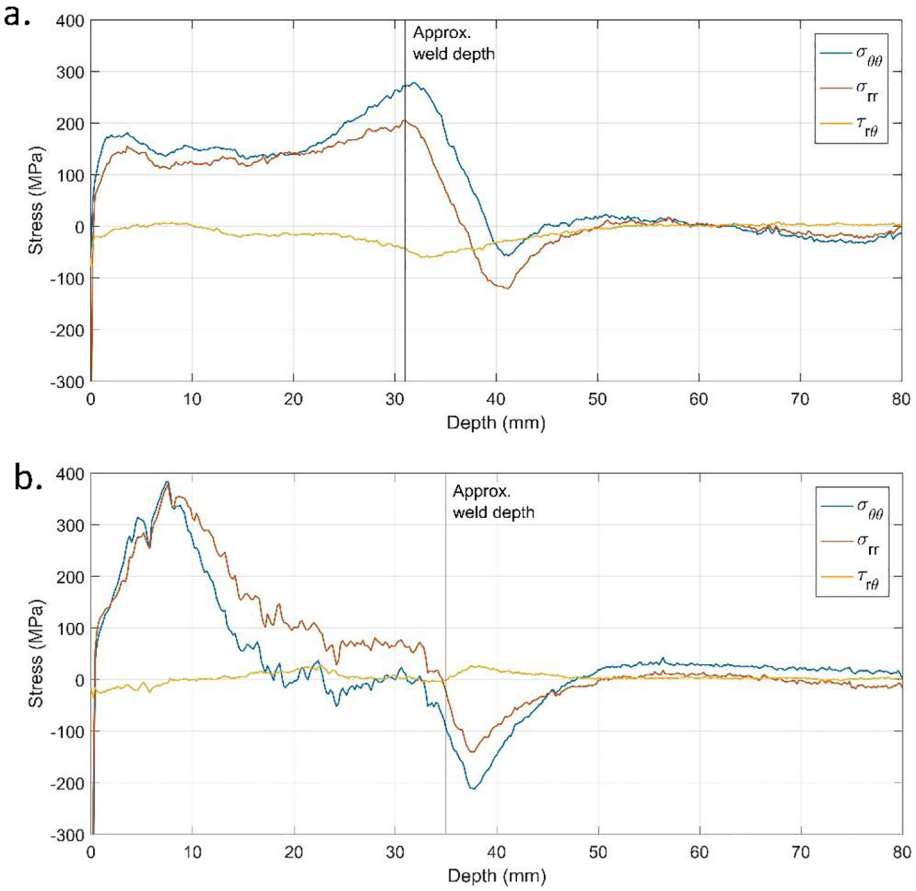

Fig. 12. Residual stress in the CRDM nozzle attachment weld. (a) Uphill measurement location. (b) Downhill measurement location.

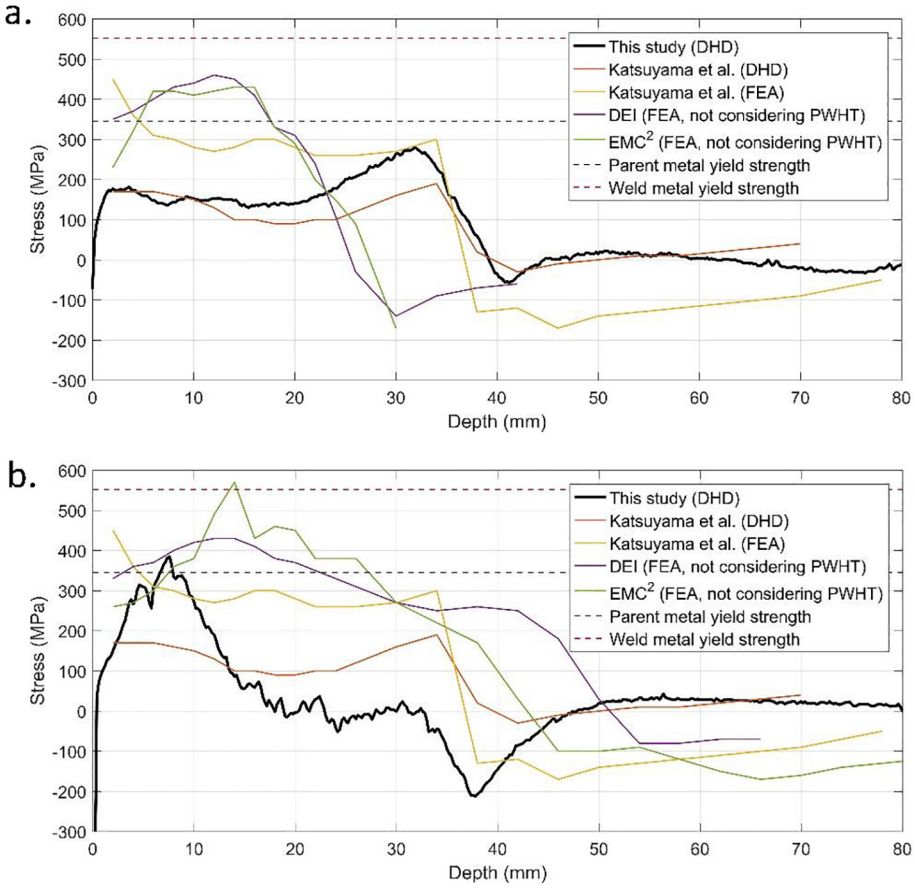

Fig. 13. Comparison of residual hoop stress in the CRDM nozzle attachment welds from different sources. (a) Uphill side, (b) downhill side. All data is for a vertical line through the attachment weld, 10 mm from the OD of the CRDM tube. Data from Katsuyama et al. (2010) is for a nozzle penetrating perpendicular to the vessel head (rather than at 40° as in the present study), after PWHT. The DEI and EMC^2 data from Rudland et al. (2007) are for a nozzle without heat treatment, penetrating at 53°.

analysis of this type of component. There is large dispersion between residual stress distributions reported for this type of weld by different sources. However, all available data suggest that for assessment purposes it would be conservative to assume that the residual hoop stress is uniformly tensile and of yield magnitude.

Acknowledgements

We gratefully acknowledge the US Nuclear Regulatory Commission for providing the specimen, and Steve Harding, Dr Karim Serasli and VEQTER Ltd. for assisting with measurements. This work was funded by the UK Engineering and Physical Sciences Research Council under grant no. EP/M019446/1 and by the Royal Academy of Engineering under a RAEng chair held by DJS.

Data statement

Data from all of the measurements discussed in this article can be downloaded from: https://doi.org/10.5523/bris.22bdwcru980cf25pu1ujwafm9g.

References

Anderson, M.T., Zhang, T., Rudland, D.L., Wilkowski, G.M., 2008. Final Report – Inspection Limit Confirmation for Upper Head Penetration Nozzle Cracking. Pacific Northwest National Laboratory PNNL-17763.

ASM Metals Handbook vol. 3, nineth ed. ASM International, 1980.

ASME Boiler and Pressure Vessel Code, Section II, Part A: Ferrous Material Specifications. American Society of Mechanical Engineers, 2001.

Bae, H.-Y., Kim, Y.-J., Kim, J.-H., Lee, S.-H., Lee, K.-S., Park, C.-Y., 2014. Three-dimensional finite element welding residual stress analysis of penetration nozzles: I – sensitivity of analysis variables. Int. J. Pressure Vessels Pip. 114–115 (1), 1–15.

Calvar, M.L., Curieres, I.D., 2012. Corrosion issues in pressurized water reactor (PWR) systems. In: Feron, D. (Ed.), Nuclear Corrosion Science and Engineering. Elsevier, pp. 473–547.

Crawford, S.L., Cinson, A.D., MacFarlan, P.J., Hanson, B.D., Mathews, R.A., 2012. Ultrasonic Phased Array Assessment of the Interference Fit and Leak Path of the North Anna Unit 2 Control Rod Drive Mechanism Nozzle 63 with Destructive Validation. United States Nuclear Regulatory Commission NUREG/CR-7142, PNNL-21547.

Fredette, L.F., 2011. Surge Nozzle NDE Specimen Mechanical Stress Improvement Analysis. PNNL NRC JCN N6319.

George, D., Kingston, E., Smith, D.J., 2002. Measurement of through-thickness stresses using small holes. J. Strain Anal. Eng. Des. 37 (2), 125–139.

Gorman, J., Hunt, S., Riccardella, P., White, G.A., 2009. In: Companion Guide to the ASME Boiler and Pressure Vessel Code, Volume 3, third ed. American Society of Mechanical Engineers, pp. 63–84 K.R. Rao, Ed.

Goudar, D.M., Truman, C.E., Smith, D.J., 2011. Evaluating uncertainty in residual stress measured using the deep-hole drilling technique. Strain 47 (1), 62–74.

Grimmel, B., 2005. U.S. Plant Experience With Alloy 600 Cracking and Boric Acid Corrosion of Light-Water Reactor Pressure Vessel Materials. U.S. Nuclear Regulatory Commission Office of Nuclear Regulatory Research NUREG-1823.

Hossain, S., Truman, C.E., Smith, D.J., 2012. Finite element validation of the deep hole drilling method for measuring residual stresses. Int. J. Pressure Vessels Pip. 93–94, 29–41.

Hwang, S.S., 2013. Review of PWSCC and mitigation management strategies of Alloy 600 materials of PWRs. J. Nucl. Mater. 443 (1–3), 321–330.

IAEA, 1999. Assessment and Management of Ageing of Major Nuclear Power Plant Components Important to Safety: PWR Pressure Vessels. International Atomic Energy Agency IAEA-TECDOC-1120.

IAEA, 2011. Stress Corrosion Cracking in Light Water Reactors: Good Practices and Lessons Learned. IAEA.

Jang, C., Lee, J., Kim, J.S., Jin, T.E., 2008. Mechanical property variation within Inconel 82/182 dissimilar metal weld between low alloy steel and 316 stainless steel. Int. J. Pressure Vessels Pip. 85, 635–646.

Kang, S.-S., Hwang, S.-S., Kim, H.-P., Lim, Y.-S., Kim, J.-S., 2014. The experience and analysis of vent pipe PWSCC (primary water stress corrosion cracking) in PWR vessel head penetration. Nucl. Eng. Des. 269, 291–298.

Katsuyama, J., Udagawa, M., Nishikawa, H., Nakamura, M., Onizawa, K., 2010. Evaluation of weld residual stress near the cladding and J-weld in reactor pressure vessel head for the assessment of PWSCC behaviour. E-J. Adv. Maint. 2, 50–64.

Kingston, E.J., 2003. Advances in the Deep-hole Drilling Technique for Residual Stress Measurement. University of Bristol.

Kingston, E.J., Stefanescu, D., Mahmoudi, A.H., Truman, C.E., Smith, D.J., 2006. Novel applications of the Deep-Hole Drilling technique for measuring through-thickness residual stress distributions. J. ASTM Int. 3 (4), JAI12568.

Mahmoudi, A.H., Hossain, S., Truman, C.E., Smith, D.J., Pavier, M.J., 2009. A new procedure to measure near yield residual stresses using the deep hole drilling technique. Exp. Mech. 49 (4), 595–604.

Mahmoudi, A.H., Truman, C.E., Smith, D.J., Pavier, M.J., 2011. The effect of plasticity on the ability of the deep hole drilling technique to measure axisymmetric residual stress. Int. J. Mech Sci. 53 (11), 978–988.

NRC, 2002. Degradation of the Davis-Besse Nuclear Power Station Reactor Pressure Vessel Head Lessons-learned Report. United States Nuclear Regulatory Commission.

Peckner, D., Bernstein, I.M. (Eds.), 1977. Handbook of Stainless Steels. McGraw-Hill.

R6: Assessment of the Integrity of Structures Containing Defects, Revision 4, Amendment 11. EDF Energy, Gloucester, 2015.

Rudland, D., Wilkowski, G., Wang, Y.-Y., Norris, W., 2004. Development of circumferential through-wall crack K-solutions for control rod drive mechanism nozzles. Int. J. Pressure Vessels Pip. 81 (12), 961–971.

Rudland, D., Wilkowski, G., Wang, Y.-Y., Norris, W., 2005. Analysis of weld residual stresses and circumferential through-wall crack K-solutions for CRDM nozzles. In: NRC Conference on Vessel Penetration Inspection, Crack Growth and Repair, pp. 161–185.

Rudland, D., Chen, Y., Zhang, T., Wilkowski, G., Broussard, J., White, G., 2007. Comparison of welding residual stress solutions for control rod drive mechanism nozzles. Proceedings of the 2007 ASME Pressure Vessels and Piping Division Conference. no. PVP2007–26045.

Sattari-Far, I., Andersson, M., 2006. "Cladding effects on structural integrity of nuclear components", Statens Kärnkraftinspektion (SKi). SKi Rep. 23.

Udagawa, M., Katsuyama, J., Onizawa, K., 2010. Study on PWSCC behaviors at nickel-based alloy welds based on weld residual stress analysis and probabilistic fracture mechanics. Proceedings of the ASME 2010 Pressure Vessels Piping Division.

Wilkowski, G., Rudland, D., Xu, H., 2006. Examination of service cracks in CRDM nozzles and relevance to flaw evaluation procedures. American Society of Mechanical Engineers, Pressure Vessels and Piping Division (Publication) PVP.